BioSystems 209 (2021) 104511

Contents lists available at ScienceDirect

BioSystems

journal homepage: www.elsevier.com/locate/biosystems

Morphology changes induced by intercellular gap junction blocking: A reaction-diffusion mechanism

Javier Cervera [a,*], Michael Levin [b], Salvador Mafe [a]

[a] Dept. Termodinàmica, Facultat de Física, Universitat de València, E-46100, Burjassot, Spain
[b] Dept. of Biology and Allen Discovery Center at Tufts University, Medford, MA, 02155-4243, USA

ARTICLE INFO

Keywords:
Morphology
Reaction-diffusion
Gap junction
Planaria
Physiological
Information

ABSTRACT

Complex anatomical form is regulated in part by endogenous physiological communication between cells; however, the dynamics by which gap junctional (GJ) states across tissues regulate morphology are still poorly understood. We employed a biophysical modeling approach combining different signaling molecules (morphogens) to qualitatively describe the anteroposterior and lateral morphology changes in model multicellular systems due to intercellular GJ blockade. The model is based on two assumptions for blocking-induced patterning: (*i*) the local concentrations of two small antagonistic morphogens diffusing through the GJs along the axial direction, together with that of an *independent*, uncoupled morphogen concentration along an orthogonal direction, constitute the instructive patterns that modulate the morphological outcomes, and (*ii*) the addition of an external agent partially blocks the intercellular GJs between neighboring cells and modifies thus the establishment of these patterns. As an illustrative example, we study how the different connectivity and morphogen patterns obtained in presence of a GJ blocker can give rise to novel head morphologies in regenerating planaria. We note that the ability of GJs to regulate the permeability of morphogens post-translationally suggests a mechanism by which different anatomies can be produced from the same genome without the modification of gene-regulatory networks. Conceptually, our model biosystem constitutes a reaction-diffusion information processing mechanism that allows reprogramming of biological morphologies through the external manipulation of the intercellular GJs and the resulting changes in instructive biochemical signals.

1. Introduction

Complex anatomical form emerges from the activity of cells during embryogenesis. While this process is extremely robust, and usually results in a species-specific stereotypical target morphology, it also exhibits considerable plasticity, as observed during regulative development and regeneration (Pinet and McLaughlin, 2019; Tung and Levin, 2020). Advances in regenerative medicine, as well as a basic understanding of evolutionary developmental biology, requires addressing important current knowledge gaps about how specific morphologies result from collective cellular activity, and what biophysical processes mediate the production of distinct outcomes from the same genomically-specified protein hardware (Pezzulo and Levin, 2015; Harris, 2018).

Theoretical approaches to morphogenesis are usually based on the pattern formation resulting from the reaction-diffusion of instructive signals (Ibañes and Izpisúa Belmonte, 2007; Lewis, 2008; Kondo and Miura, 2010; Green and Sharpe, 2015). While the propagation of these signals may involve the cellular uptake of specific molecules from the external microenvironment, it can also occur through intercellular mechanisms, e.g. using gap junctions (GJs) between adjacent cells (Mathews and Levin, 2017; Emmons-Bell et al., 2015; Glen et al., 2018). Gap junctions are versatile signaling gates that enable many cell types to form communicating networks with complex signaling and computational capacities (Palacios-Prado and Bukauskas, 2009; Li et al., 2018; Seki et al., 2014; Cervera et al., 2019; Bhattacharya et al., 2020). To begin to understand how the dynamics of GJ signaling can be mapped onto large-scale anatomical (system-level) outcomes, we constructed and analyzed a biophysical model combining two antagonistic (coupled) signaling molecules and another (uncoupled) orthogonal one to describe the anteroposterior and lateral morphology changes observed in a multicellular system after intercellular GJ blocking.

Our model does not invoke any specific morphogen and intercellular blocker but we believe that the basic concepts introduced are of

* Corresponding author.
E-mail address: javier.cervera@uv.es (J. Cervera).

https://doi.org/10.1016/j.biosystems.2021.104511
Received 30 July 2021; Accepted 14 August 2021
Available online 17 August 2021

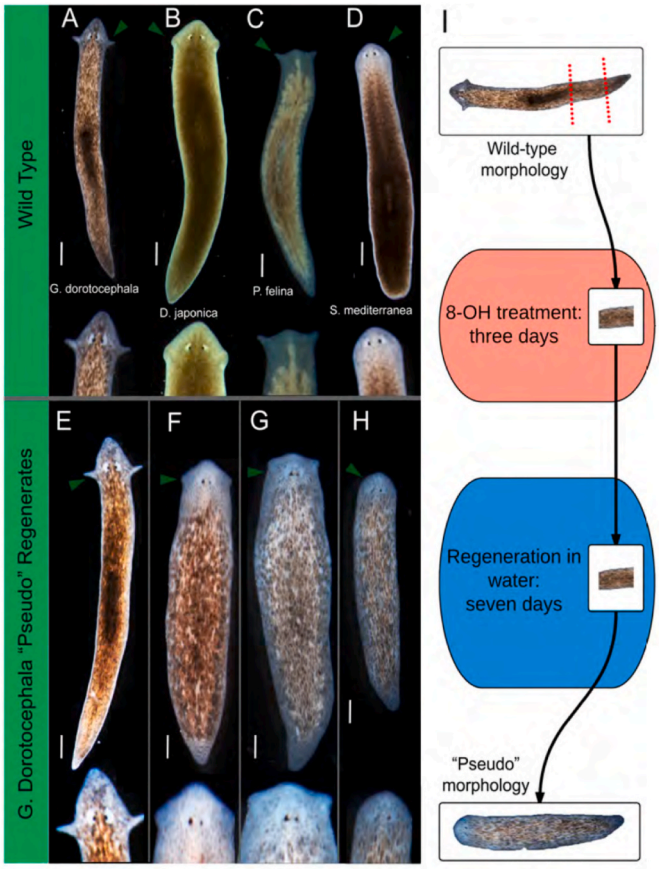

Fig. 1. Different head morphologies observed after octanol treatment of four species of planaria flatworm (A–D). The arrows indicate the distinct head shapes (E–H) obtained when the pre-tail fragments are amputated from *G. dorotocephala* worms and treated according to the experimental procedure shown in the figure. The scale bar corresponds to 0.5 mm. Adapted from Emmons-Bell et al. (2015).

qualitative interest for describing the blocking effect of external agents on intercellular communication via numerous possible mediating molecules (including neurotransmitters, calcium, other ions, and small metabolites (Esser et al., 2006; Fukumoto et al., 2005; Gairhe et al., 2012)). Since junctional blocking can lead to changes in the permeability of GJs to different types of small signaling molecules that impact morphogenesis, we propose a simple framework for understanding how GJ manipulation gives rise to diverse morphotypes of complex anatomical features. As an illustrative case, we focus on the ability of exposure to octanol (Fig. 1), a gap junction blocker, to induce head shapes in planarian flatworms that belong to other species of planaria (Emmons-Bell et al., 2015).

Planarian flatworms are a popular model for understanding the regulation of growth and form (Saló et al., 2009; Cebrià et al., 2018). When cut into fragments, each piece restores exactly what is missing to make a complete worm, challenging the community to understand the algorithms that enable cells to work towards a specific anatomical outcome and stop when that target morphology is finished (Pezzulo and Levin, 2016; Harris, 2018). Understanding this process has implications not only for the origin and regulation of body form, but also for new approaches to regenerative medicine (Ingber and Levin, 2007; Rando, 2014). While significant insight exists into the determinants of the number and location(s) of heads (Petersen and Reddien, 2007; Iglesias et al., 2008; Umesono et al., 2013; Owlarn and Bartscherer, 2016; Durant et al., 2019; Pietak et al., 2019; Bischof et al., 2020), less information is available about what factors determine the shape of the heads observed in different species of planaria. Interestingly, experiments revealed that wild-type (genomically-normal) planarian cells can be induced to build heads appropriate to other species of planaria (Emmons-Bell et al., 2015). Using octanol, a blocker of electrical synapses known as GJs (Adler and Woodruff, 2000) that reduces physiological connectivity during regeneration, it was observed that head shapes (including characteristic brain shape and distributions of stem cells) were produced that closely resemble those of other extant planarian species.

Previous modeling efforts have addressed the bioelectrical cell- and tissue-level dynamics that regulate the location of heads (Levin et al., 2019; Cervera et al., 2020) and the cellular control signals that could give rise to diverse head shapes (Bessonov et al., 2015; Emmons-Bell et al., 2015; Tosenberger et al., 2015). It is now necessary to complement these aspects with biochemical gradients known to implement body-plan information, in order to explain the varieties of head morphotypes that can be produced by genetically-normal cells. We make use of a theoretical approach to development based on pattern formation and instructive signals (Müller and El-Sherif, 2020). First, we consider a system of reaction-diffusion equations describing two oppositely directed morphogen gradients with an annihilation term (McHale et al., 2006) as a qualitative explanation to the anteroposterior morphology (Emmons-Bell et al., 2015). Because antagonistic morphogens and local mutual inhibition have previously been related to the head-tail polarity of multicellular systems, our approach should have both experimental (Houchmandzadeh et al., 2005; Niehrs, 2010; Stückemann et al., 2017; Čapek and Müller, 2019; Durant et al., 2019) and theoretical (McHale et al., 2006) plausibility. In particular, the long-time action of blastema depolarization on planaria antero-posterior polarity has been related with the local mutual inhibition by Notum and β-catenin (Durant et al., 2019). Second, we extend the above approach to the case of a third morphogen diffusing independently along an orthogonal direction that modulates the lateral geometry (Niehrs, 2010).

Experimentally, long-range signaling gradients and auto-regulatory feedback mechanisms are required to modulate polarity and lateral development during model systems regeneration (Niehrs, 2010; Sullivan et al., 2016; Stückemann et al., 2017; Čapek and Müller, 2019). Theoretically, these processes cannot rely on simple Turing mechanisms only because of the need to avoid repeated patterns while keeping the scaling constraints of a size-invariant developing field (McHale et al., 2006; Umulis and Othmer, 2013; Čapek and Müller, 2019). We propose that it is the combined action of orthogonal morphogen gradients along the x and z axes that give rise to the different head shapes observed in absence and presence of GJ blockers. For the particular case of planaria tissues, a complete review of biophysical and computational approaches has recently been presented (see Levin et al., 2019 and references therein) together with comprehensive models focused on complex regeneration processes (Werner et al., 2015; Harris 2018; Pietak et al., 2019; Herath and Lobo, 2020). Our qualitative approach is focused on simple but versatile biophysical concepts which are not restricted to the simulation of any specific system, morphogen, intercellular blocker, or genetic spatial gradient.

2. Biophysical model

Biological systems operate under a hierarchy of time scales characteristic of electrical, mechanical, diffusional, and transcriptional processes. Different mechanisms can lead to scale invariance in the formation of spatial patterns (McHale et al., 2006; Umulis, and Othmer, 2013; Čapek and Müller, 2019) and many biochemical agents can influence the observed morphological outcomes (Owlarn and Bartscherer, 2016; Stückemann et al., 2017; Čapek and Müller, 2019). Here, we will focus on the diffusional regime of two generic small morphogens along the axial direction and assume that their local concentrations are representative of the instructive spatial patterns that modulate the system polarity (Stückemann et al., 2017; Čapek and Müller, 2019). In particular, we use first the reaction-diffusion approach by McHale et al.

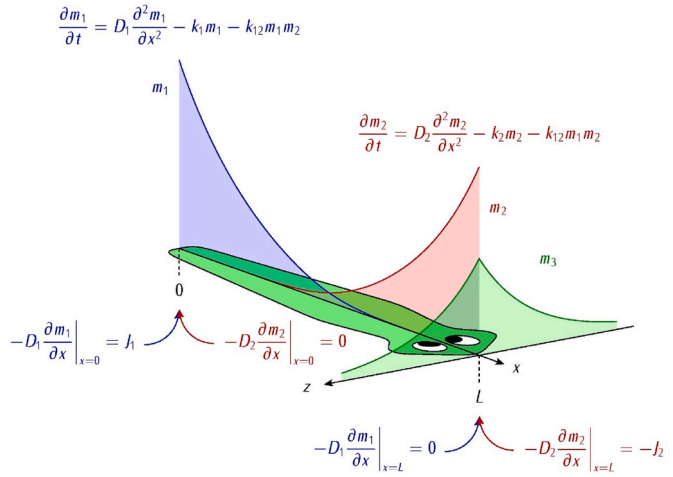

Fig. 2. The spatial regionalization of the two small morphogen concentrations m_1 and m_2 along the x axis establishes the anteroposterior morphology of the multicellular system considered here. We neglect the diffusion of these two morphogens along the orthogonal z axis and solve the reaction-diffusion equations with appropriate boundary conditions at the axial positions $x = 0$ (tail) and L (head) assuming a constant length L characteristic of the system size. Note that the morphogen production fluxes J_1 and J_2 point towards the center of the system (McHale et al., 2006). The model equations can be put in dimensionless form by introducing the decay lengths $\lambda_i = (D_i/k_i)^{1/2} = [D_i/(k_{12}m_0)]^{1/2}$, $i = 1$ and 2, where m_0 is a reference morphogen concentration. Because the position of the central wavefront between the two morphogen concentrations is regulated by the respective lengths λ_i, the different changes in the diffusion coefficients $D_1$and D_2 caused by GJ blocking will eventually impact on the morphogen spatial patterns. For the sake of completeness, we introduce also a third morphogen of concentration m_3 that diffuses independently of the former two only along the orthogonal direction (z axis), being relevant to lateral morphology (Niehrs, 2010; Ivankovic et al., 2019). This introduction is only formal because we will focus on the antagonistic coupling of the axial morphogens 1 and 2 (Stückemann et al., 2017; Čapek and Müller, 2019) here. In fact, the role of this morphogen could also be played by a double longitudinal and orthogonal gradient of the second morphogen.

(2006) for two antagonistic morphogens because of its biological plausibility and scaling properties (Stückemann et al., 2017; Čapek and Müller, 2019; Ivankovic et al., 2019).

We consider further that a generic blocker, e.g. octanol, partially blocks the intercellular GJ between neighboring cells, as observed experimentally (Emmons-Bell et al., 2015; Sullivan et al., 2016). In planarian tissues, this blocking should give a statistical distribution of decreased GJs pore radii that will eventually result in lower diffusion coefficients D_i for the morphogens $i = 1$ and 2 due to their increased hindrance with the pore surface (Dechadilok and Deen, 2006; Stroeve et al., 2014; Eloul and Compton, 2016). Crucially, due to the *distinct* morphogen sizes and effective radii, the diffusion coefficients D_1 and D_2 must be affected to *different* degrees upon GJ blocking (Dechadilok and Deen, 2006; Eloul and Compton, 2016). Because the morphogens concentrations m_1 and m_2 that regulate development depend on the relative values of D_1 and D_2 (Houchmandzadeh et al., 2005; McHale et al., 2006), it is conceivable that intercellular blocking will affect head morphologies (Emmons-Bell et al., 2015; Sullivan et al., 2016). Although our theoretical approach is based on two antagonistic morphogens that could be related to the anteroposterior axial polarity (Stückemann et al., 2017; Čapek and Müller, 2019; Ivankovic et al., 2019), we introduce also a third morphogen that diffuses along an orthogonal direction because of its experimental relevance to lateral morphology (Niehrs, 2010).

We consider first the reaction-diffusion equations describing the change of concentrations m_1 and m_2 with time t together with the system boundary conditions (Fig. 2). Diffusion, degradation, and annihilation

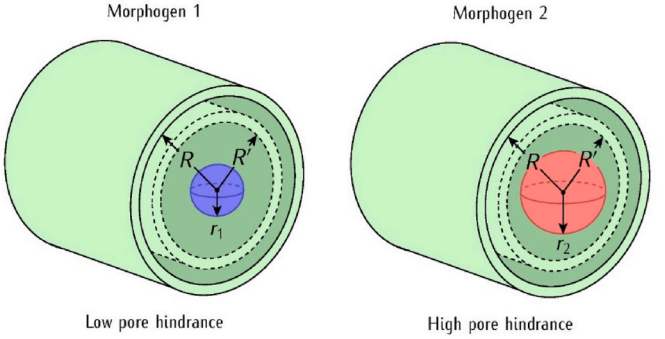

Fig. 3. The blocking decreases the GJ radius down to an effective value $R' < R$. This partial pore blocking makes the diffusion coefficient of the bulkier morphogen 2 to decrease to a new effective value $D_2' = D_2F\left(\frac{r_2}{R'}\right) < D_2$ because of the hindrance factor $F\left(\frac{r_2}{R'}\right) < 1$. On the contrary, we assume that the diffusion coefficient of morphogen 1 is not significantly affected because of its small size ($r_1 < r_2$) and thus $D_1' = D_1F\left(\frac{r_1}{R'}\right) = D_1$ as a first approximation. Consequently, the new decay lengths are $\lambda_2' < \lambda_2$ for morphogen 2 and $\lambda_1' = \lambda_1$ for morphogen 1.

terms are included. The first term is modulated by the diffusion coefficients D_1 and D_2. The second term expresses the morphogen consumptions that are characterized by the rate constants k_1 and k_2. The third term corresponds to an effective annihilation process of rate constant k_{12} that couples the morphogen concentrations m_1 and m_2. This term quantifies the morphogens antagonism through their mutual inhibition without assuming any particular binding reaction to each other.

For the multicellular system of Fig. 2, the mechanisms that can generate possible head shapes result from the interplay between the local concentrations and gradients of the different morphogens (Meinhardt, 2009; Adell et al., 2010; Lander and Petersen, 2016; Stückemann et al., 2017; Čapek and Müller, 2019; Ivankovic et al., 2019; Herath and Lobo, 2020). Thus, the morphogenetic activity that leads to the model system shape is modulated by: (*i*) the morphogen production fluxes J_i, (*ii*) the degradation k_i and annihilation k_{12} rate constants, and (*iii*) the diffusion coefficients D_i. In particular, the position of the wavefront between the morphogen concentrations of Fig. 2, regulated by the decay lengths λ_i and the system length L, is crucial to the antero-posterior shape (McHale et al., 2006). Note that this position should be modified by the GJ blocking because of the resulting changes in the diffusion coefficients.

We introduce now the effect of blocking (Fig. 3) on the instructive multicellular patterns of Fig. 2 assuming that it acts to decrease the GJ radius R down to an effective value $R' < R$. In general, morphogens 1 and 2 will have different sizes and effective diffusional radii $r_1 < r_2$. Conceivably, the partial GJ blocking shown in Fig. 3 will slow down the bulkier morphogen 2 because the dimensionless hindrance factor $F\left(\frac{r_i}{R'}\right) < 1$ that decreases the diffusion coefficient D_i depends on the relative radii r_i/R', $i = 1$ and 2 (Dechadilok and Deen, 2006; Eloul and Compton, 2016). Note that this phenomenological hindrance factor indirectly accounts for steric and electrical charge effects (Stroeve et al., 2014). On the contrary, the degradation constants k_1 and k_2 and the production fluxes J_1 and J_2 should not be affected by the GJ blocking. The *different* decreases in the morphogen diffusion coefficients obtained upon blocking (Fig. 3) will give *distinct* decreases in the respective decay lengths of the concentration patterns of morphogens 1 and 2 of Fig. 2. In relative terms, we consider that $\lambda_2' < \lambda_2$ for morphogen 2 while $\lambda_1' = \lambda_1$ for morphogen 1 upon blocking.

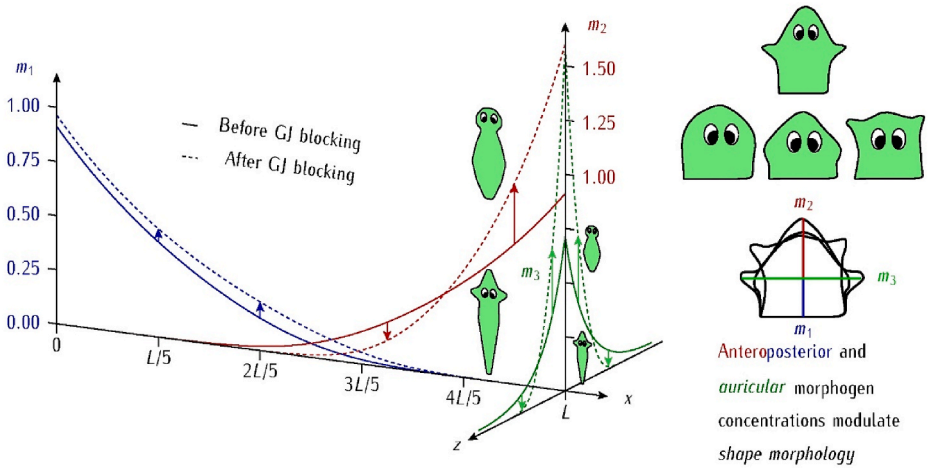

Fig. 4. The position of the central wavefront between the morphogen axial concentrations m_1 and m_2 scaled to a reference concentration m_0 depends markedly on the respective decay lengths λ_1 and λ_2 (*left*). Thus, any change in the diffusion coefficients D_1 and D_2 caused by the GJ blocking should impact on the morphogen spatial patterns (*arrows*) of the multicellular system, as shown schematically (*insets*). The different changes in the instructive patterns provided by the anteroposterior morphogens 1 and 2 and the auricular morphogen 3 resulting from the GJ blocking lead to the distinct expression patterns and head shapes (*right*) of Fig. 1 (Emmons-Bell et al., 2015). The morphogen concentrations are obtained under steady state conditions (zero time derivatives) assuming the dimensionless production fluxes $J_i/(D_i m_0/L) = 1$ $(i = 1, 2)$, $k_1/k_2 = 1$ in the respective decay lengths λ_1 and λ_2, and $k_{12} = 100(k_1/m_0)$ (see Fig. 2). For morphogen 1, we assume $\lambda_1(\text{continuous curve}) = \lambda_1'$ (dashed curve) $= L/3$ while for morphogen 2, $\lambda_2(\text{continuous curve}) = L/3$ and $\lambda_2'(\text{dashed curve}) = L/5$. For this choice of parameters, the new diffusion coefficients after blocking (*dashed* curves) are $D_1' = D_1$ and $D_2' = F\left(\frac{r_2}{R'}\right)D_2 = \left(\frac{9}{25}\right)D_2$. For the uncoupled morphogen of concentration m_3 (scaled also to the reference concentration m_0) which diffuses independently along the z axis, we assume also a reaction-diffusion scheme (Fig. 2) with no mutual annihilation term. In this case, we introduce the decreased diffusion coefficient $D_3' < D_3$ upon blocking and show schematically the resulting concentration shift from m_3 (*continuous* curve) to m_3' (*dashed* curve). Note that other choices of parameters showing similar qualitative trends are possible.

3. Results and discussion

Fig. 4 shows the effects of GJ blocking on the morphogen decay lengths and concentrations schematically shown in Fig. 2. The antagonistic concentrations m_1 and m_2 are coupled along the x axis to regulate the anteroposterior head-tail polarity of the multicellular system. When combined with a third morphogen concentration m_3 that diffuses independently along the orthogonal z axis to regulate the lateral (auricular) geometry (Fig. 4), they give rise to the particular head morphology (Emmons-Bell et al., 2015; Sullivan et al., 2016). Alternatively, a double longitudinal and orthogonal gradient of the second morphogen could also be used. Our study is focused on the possible role of GJ blocking and suggests that the resulting changes in the signaling molecules gradients lead to the different instructive patterns that will eventually give the distinct morphological outcomes schematically shown in Fig. 4.

Upon GJ blocking, a significant shift in the reaction wavefront of the concentrations m_1 and m_2 along the x axis is obtained because of the new axial concentration m_2' resulting from the new condition $D_2' < D_2$ (Fig. 3). In addition, the morphogen concentration m_3 can also be affected by the GJ blocking because of the decreased diffusion coefficient $D_3' < D_3$ leading to a new orthogonal concentration m_3' along the z axis, as shown schematically in Fig. 4 (*left*). Conceivably, the spatial shifts in the morphogen concentrations and gradients along the x and z axes obtained upon GJ blocking should be related to the different instructive patterns, which will eventually result in distinct expression patterns and head shapes compared with that obtained in absence of blocking (Fig. 4, *right*). In the case of planarian flatworms, the absence of polarity could be ascribed to the dominant role and finite availability of one of the morphogens throughout the system (Adell et al., 2010). Also, the different outcomes achieved after amputation and subsequent GJ blocking (Fig. 1) could be explained by the distinct morphogen local concentrations and stochastic blocking patterns characteristic of each regenerating fragment (Adell et al., 2010; Emmons-Bell et al., 2015; Lander and Petersen, 2016).

We must make it clear that we have not described the time dependent regeneration process here: Fig. 4 (*left*) shows the steady state morphogen concentrations established over a fixed system size L. In principle, the model equations of Fig. 2 are time-dependent and could then be rewritten for the case of a time varying size $L(t)$ in order to describe the effects of blocking on the *spatio-temporal* instructive patterns that lead to the different morphotypes of Fig. 1. We have not considered this case, but it is plausible that an *externally-modulated timing* of GJ opening and closing may also affect regeneration because of the concomitant changes in these patterns. Although more realistic and complex models have been presented (Werner et al., 2015; Pietak et al., 2019; Herath and Lobo, 2020), we have tried to emphasize here the specific reaction and diffusional system parameters (Fig. 2) to tinker in order to obtain the distinct morphologies (Fig. 1). In this context, our approach provides useful qualitative concepts that can be extended further. For instance, the effect of the GJ blocking on the diffusion coefficients described here could now be extended to the case of the electrophoretic transport of signaling ions and charged molecules (Esser et al., 2006) that regulate the electrical potential patterns (Cervera et al., 2020) in the multicellular system. We note also that the morphology changes could be reversible if washing-out of the blocker in water eventually reestablishes the intercellular communication and the correct morphogen concentration gradients (Emmons-Bell et al., 2015).

4. Conclusions

We have employed a biophysical approach combining two antagonistic signaling molecules (morphogens) and one independent orthogonal morphogen to qualitatively describe the anteroposterior and lateral morphology changes of model multicellular systems after intercellular GJ blocking. To this end, we have introduced two biologically plausible assumptions: (*i*) the local concentrations of two small morphogens along the axial direction, together with that of a third morphogen concentration along an orthogonal direction, may constitute the instructive patterns that modulate the morphological outcomes (Niehrs, 2010; Čapek and Müller, 2019; Durant et al., 2019; Ivankovic et al., 2019) and (*ii*) the addition of an external agent partially blocks the intercellular GJs between neighboring cells that allow the morphogens diffusion and modifies thus these patterns (Emmons-Bell et al., 2015; Sullivan et al., 2016). In particular, the first assumption can be related to existing mechanistic work on anterior-posterior (Adell et al., 2010; Evans et al., 2011; Agata et al., 2014) and medio-lateral (Saito et al., 2003; Gurley

et al., 2010) patterning in regenerating planaria.

Because of the distinct morphogen sizes and effective radii, the partial GJ blocking should affect their diffusion coefficients differently. Clearly, the different decreases produced in these diffusion coefficients after blocking will eventually lead to the corresponding changes in the decay lengths that modulate the morphogen concentrations in the axial (Houchmandzadeh et al., 2005; McHale et al., 2006) and orthogonal directions (Fig. 4). We suggest that the different instructive patterns obtained in presence of GJ blocking will give rise to distinct head morphologies compared with those observed in absence of blocking, as observed in planaria (Emmons-Bell et al., 2015; Sullivan et al., 2016). Note that while we illustrate our model dynamics in one particular biological system (Figs. 1 and 2), we have not tied this model to any specific morphogen and intercellular blocker nor described the time-dependent regeneration process here. Also, although we have assumed a set of generic morphogens to be the agents disturbed by GJ blocking, other impeded intercellular signals could alternatively be invoked (Emmons-Bell et al., 2015; Pietak et al., 2019). Despite these evident limitations, the basic concepts introduced can be useful to incorporate the effect of GJ blocking in more complex regulatory mechanisms and expression gradients (Meinhardt, 2009; Adell et al., 2010; Emmons-Bell et al., 2015; Werner et al., 2015; Lander and Petersen, 2016; Pietak et al., 2019; Herath and Lobo, 2020).

As future work, we may mention the integration of the biochemical gradients with the bioelectrical spatial regionalization (Cervera et al., 2020) that influences also the body-plan information. Also, given the ability of octanol to produce regenerated head shapes characteristic of other planaria species (Emmons-Bell et al., 2015), we may characterize further the particular GJ properties among these species. The future development of techniques to track spatial patterns of GJ permeability *in vivo* would help to reveal the ways in which evolution can tune GJ-dependent processes to produce diverse morphotypes. In conclusion, we believe that the ability of GJs to regulate the permeability of signaling molecules and ions post-translationally (Emmons-Bell et al., 2015; Cervera et al., 2017; Glen et al., 2018) suggests an important mechanism by which different anatomies can be produced from the same genome, by acting on physiological signals that do not require modifications in the morphogen properties or specific gene-regulatory networks. In this context, our model biosystem could be regarded as a reaction-diffusion processor (Adamatzky et al., 2005) that allows reprogramming biological morphologies through the external manipulation of the intercellular GJs and the resulting changes in instructive biochemical signals.

Declaration of competing interest

The authors declare that they have no known competing financial interests or personal relationships that could have appeared to influence the work reported in this paper.

Acknowledgments

J. C. and S. M. acknowledge the *Ministerio de Ciencia e Innovación* (Spain) and the European Regional Development Funds (FEDER), project No. PGC2018-097359-B-I00. M. L. acknowledges the support by an Allen Discovery Center award from The Paul G. Allen Frontiers Group (No. 12171), the Templeton World Charity Foundation (TWCF0089/AB55), the Barton Family Foundation, the Guy Foundation Family Trust, and the Defense Advanced Research Projects Agency (DARPA) under Cooperative Agreement Number HR0011-18-2-0022 (the content of the information does not necessarily reflect the position or the policy of the Government, and no official endorsement should be inferred).

References

Adamatzky, A., Costello, B.D.L., Asai, T., 2005. Reaction-Diffusion Computers. Elsevier, New York.
Adell, T., Cebrià, F., Salo, E., 2010. Gradients in planarian regeneration and homeostasis. Cold Spring Harb. Perspect. Biol. 2, a000505.
Adler, E.L., Woodruff, R.I., 2000. Varied effects of 1-octanol on gap junctional communication between ovarian epithelial cells and oocytes of Oncopeltus fasciatus, Hyalophora cecropia, and Drosophila melanogaster. Arch. Insect Biochem. Physiol. 43, 22–32.
Agata, K., Tasaki, J., Nakajima, E., Umesono, Y., 2014. Recent identification of an ERK signal gradient governing planarian regeneration. Zoology 117, 161–162.
Bessonov, N., Levin, M., Morozova, N., Reinberg, N., Tosenberger, A., Volpert, V., 2015. On a model of pattern regeneration based on cell memory. PloS One 10, e0118091.
Bhattacharya, S., Hyland, C., Falk, M.M., Iovine, M.K., 2020. Connexin 43 gap junctional intercellular communication inhibits evx1 expression and joint formation in regenerating fins. Development 147, dev190512.
Bischof, J., Day, M.E., Miller, K.A., LaPalme, J., Levin, M., 2020. Nervous system and tissue polarity dynamically adapt to new morphologies in planaria. Dev. Biol. 467, 51–65.
Čapek, D., Müller, P., 2019. Positional information and tissue scaling during development and regeneration. Development 146, dev177709.
Cebrià, F., Adell, T., Saló, E., 2018. Rebuilding a planarian: from early signaling to final shape. Int. J. Dev. Biol. 62, 537–550.
Cervera, J., Meseguer, S., Mafe, S., 2017. MicroRNA intercellular transfer and bioelectrical regulation of model multicellular ensembles by the gap junction connectivity. J. Phys. Chem. B 121, 7602–7613.
Cervera, J., Pai, V.P., Levin, M., Mafe, S., 2019. From non-excitable single-cell to multicellular bioelectrical states supported by ion channels and gap junction proteins: electrical potentials as distributed controllers. Prog. Biophys. Mol. Biol. 149, 39–53.
Cervera, J., Meseguer, S., Levin, M., Mafe, S., 2020. Bioelectrical model of head-tail patterning based on cell ion channels and intercellular gap junctions. Bioelectrochemistry 132, 107410.
Dechadilok, P., Deen, W.M., 2006. Hindrance factors for diffusion and convection in pores. Ind. Eng. Chem. Res. 45, 6953–6959.
Durant, F., Bischof, J., Fields, C., Morokuma, J., LaPalme, J., Hoi, A., Levin, M., 2019. The role of early bioelectric signals in the regeneration of planarian anterior/posterior polarity. Biophys. J. 116, 948–961.
Eloul, S., Compton, R.G., 2016. General model of hindered diffusion. J. Phys. Chem. Lett. 7, 4317–4321.
Emmons-Bell, M., Durant, F., Hammelman, J., Bessonov, N., Volpert, V., Morokuma, J., Pinet, K., Adams, D.S., Pietak, A., Lobo, D., Levin, M., 2015. Gap junctional blockade stochastically induces different species-specific head anatomies in genetically wild-type Girardia dorotocephala flatworms. Int. J. Mol. Sci. 16, 27865–27896.
Esser, A.T., Smith, K.C., Weaver, J.C., Levin, M., 2006. Mathematical model of morphogen electrophoresis through gap junctions. Dev. Dynam. 235, 2144–2159.
Evans, D.J., Owlarn, S., Tejada Romero, B., Chen, C., Aboobaker, A.A., 2011. Combining classical and molecular approaches elaborates on the complexity of mechanisms underpinning anterior regeneration. PloS One 6, e27927.
Fukumoto, T., Kema, I.P., Levin, M., 2005. Serotonin signaling is a very early step in patterning of the left-right axis in chick and frog embryos. Curr. Biol. 15, 794–803.
Gairhe, S., Bauer, N.N., Gebb, S.A., McMurtry, I.F., 2012. Serotonin passes through myoendothelial gap junctions to promote pulmonary arterial smooth muscle cell differentiation. Am. J. Physiol. Lung Cell Mol. Physiol. 303, L767–L777.
Glen, C.M., McDevitt, T.C., Kemp, M.L., 2018. Dynamic intercellular transport modulates the spatial patterning of differentiation during early neural commitment. Nat. Commun. 9, 4111.
Green, J.B.A., Sharpe, J., 2015. Positional information and reaction-diffusion: two big ideas in developmental biology combine. Development 142, 1203–1211.
Gurley, K.A., Elliott, S.A., Simakov, O., Schmidt, H.A., Holstein, T.W., Sanchez Alvarado, A., 2010. Expression of secreted Wnt pathway components reveals unexpected complexity of the planarian amputation response. Dev. Biol. 347, 24–39.
Harris, A.K., 2018. The need for a concept of shape homeostasis. Biosystems 173, 65–72.
Herath, S., Lobo, D., 2020. Cross-inhibition of Turing patterns explains the self-organized regulatory mechanism of planarian fission. J. Theor. Biol. 485, 110042.
Houchmandzadeh, B., Wieschaus, E., Leibler, S., 2005. Precise domain specification in the developing Drosophila embryo. Phys. Rev. E 72, 061920.
Ibañes, M., Izpisúa Belmonte, J.C., 2007. Theoretical and experimental approaches to understand morphogen gradients. Mol. Syst. Biol. 4, 176.
Iglesias, M., Gomez-Skarmeta, J.L., Saló, E., Adell, T., 2008. Silencing of Smed-betacatenin1 generates radial-like hypercephalized planarians. Development 135, 1215–1221.
Ingber, D.E., Levin, M., 2007. What lies at the interface of regenerative medicine and developmental biology? Development 134, 2541–2547.
Ivankovic, M., Haneckova, R., Thommen, A., Grohme, M.A., Vila-Farré, M., Werner, S., Rink, J.C., 2019. Model systems for regeneration: planarians. Development 146, dev167684.
Kondo, S., Miura, T., 2010. Reaction-diffusion model as a framework for understanding biological pattern formation. Science 329, 1616–1620.
Lander, R., Petersen, C.P., 2016. Wnt, Ptk7, and FGFRL expression gradients control trunk positional identity in planarian regeneration. Elife 5, e12850.
Levin, M., Pietak, A., Bischof, J., 2019. Planarian regeneration as a model of anatomical homeostasis: recent progress in biophysical and computational approaches. Semin. Cell Dev. Biol. 87, 125–144.

Lewis, J., 2008. From signals to patterns: space, time, and mathematics in developmental biology. Science 322, 399–403.
Li, A., Cho, J.H., Reid, B., Tseng, C.C., He, L., Tan, P., Yeh, C.Y., Wu, P., Li, Y., Widelitz, R.B., Zhou, Y., Zhao, M., Chow, R.H., Chuong, C.M., 2018. Calcium oscillations coordinate feather mesenchymal cell movement by SHH dependent modulation of gap junction networks. Nat. Commun. 9, 5377.
Mathews, J., Levin, M., 2017. Gap junctional signaling in pattern regulation: physiological network connectivity instructs growth and form. Dev. Neurobiol. 77, 643–673.
McHale, P., Rappel, W.J., Levine, H., 2006. Embryonic pattern scaling achieved by oppositely directed morphogen gradients. Phys. Biol. 3, 107–120.
Meinhardt, H., 2009. Beta-catenin and axis formation in planarians. Bioessays 31, 5–9.
Müller, P., El-Sherif, E., 2020. A systems-level view of pattern formation mechanisms in development. Dev. Biol. 460, 1.
Niehrs, C., 2010. On growth and form: a Cartesian coordinate system of Wnt and BMP signaling specifies bilaterian body axes. Development 137, 845–857.
Owlarn, S., Bartscherer, K., 2016. Go ahead, grow a head! A planarian's guide to anterior regeneration. Regeneration (Oxf) 3, 139–155.
Palacios-Prado, N., Bukauskas, F.F., 2009. Heterotypic gap junction channels as voltage-sensitive valves for intercellular signaling. Proc. Natl. Acad. Sci. U. S. A. 106, 14855–14860.
Petersen, C.P., Reddien, P.W., 2007. Smed-{beta}catenin-1 is required for anteroposterior blastema polarity in planarian regeneration. Science 319, 327–330.
Pezzulo, G., Levin, M., 2015. Re-membering the body: applications of computational neuroscience to the top-down control of regeneration of limbs and other complex organs. Integr. Biol. (Camb). 7, 1487–1517.
Pezzulo, G., Levin, M., 2016. Top-down models in biology: explanation and control of complex living systems above the molecular level. J. R. Soc. Interface 13, 20160555.
Pietak, A., Bischof, J., LaPalme, J., Morokuma, J., Levin, M., 2019. Neural control of body-plan axis in regenerating planaria. PLoS Comput. Biol. 15, e1006904.
Pinet, K., McLaughlin, K.A., 2019. Mechanisms of physiological tissue remodeling in animals: manipulating tissue, organ, and organism morphology. Dev. Biol. 451, 134–145.
Rando, T.A., 2014. Regenerative medicine: of fish and men. Nat. Chem. Biol. 10, 91–92.
Saito, Y., Koinuma, S., Watanabe, K., Agata, K., 2003. Mediolateral intercalation in planarians revealed by grafting experiments. Dev. Dynam. 226, 334-334.
Saló, E., Abril, J.F., Adell, T., Cebrià, F., Eckelt, K., Fernandez-Taboada, E., Handberg-Thorsager, M., Iglesias, M., Molina, M.D., Rodriguez-Esteban, G., 2009. Planarian regeneration: achievements and future directions after 20 years of research. Int. J. Dev. Biol. 53, 1317–1327.
Seki, A., Nishii, K., Hagiwara, N., 2014. Gap junctional regulation of pressure, fluid force, and electrical fields in the epigenetics of cardiac morphogenesis and remodeling. Life Sci. 129, 27–34.
Stroeve, P., Rahman, M., Naidu, L.D., Chu, G., Mahmoudi, M., Ramirez, P., Mafe, S., 2014. Protein diffusion through charged nanopores with different radii at low ionic strength. Phys. Chem. Chem. Phys. 16, 21570–21576.
Stückemann, T., Cleland, J.P., Werner, S., Thi-Kim, V.H., Bayersdorf, R., Liu, S.Y., Friedrich, B., Jülicher, F., Rink, J.C., 2017. Antagonistic self-organizing patterning systems control maintenance and regeneration of the anteroposterior Axis in planarians. Dev. Cell 40, 248–263.
Sullivan, K.G., Emmons-Bell, M., Levin, M., 2016. Physiological inputs regulate species-specific anatomy during embryogenesis and regeneration. Commun. Integr. Biol. 9, e1192733.
Tosenberger, A., Bessonov, N., Levin, M., Reinberg, N., Volpert, V., Morozova, N., 2015. A conceptual model of morphogenesis and regeneration. Acta Biotheor. 63, 283–294.
Tung, A., Levin, M., 2020. Extra-genomic instructive influences in morphogenesis: a review of external signals that regulate growth and form. Dev. Biol. 461, 1–12.
Umesono, Y., Tasaki, J., Nishimura, Y., Hrouda, M., Kawaguchi, E., Yazawa, S., Nishimura, O., Hosoda, K., Inoue, T., Agata, K., 2013. The molecular logic for planarian regeneration along the anterior-posterior axis. Nature 500, 73–76.
Umulis, D.M., Othmer, H.G., 2013. Mechanisms of scaling in pattern formation. Development 140, 4830–4843.
Werner, S., Stückemann, T., Beirán Amigo, M., Rink, J.C., Jülicher, F., Friedrich, B.M., 2015. Scaling and regeneration of self-organized patterns. Phys. Rev. Lett. 114, 138101.